Selective metathesis synthesis of MgCr$_2$S$_4$ by control of thermodynamic driving forces

Akira Miura,[a*] Hiroaki Ito,[b] Christopher J. Bartel,[c] Wenhao Sun,[d*] Nataly Carolina Rosero-Navarro,[a] Kiyoharu Tadanaga,[a] Hiroko Nakata,[e] Kazuhiko Maeda,[e] Gerbrand Ceder[c,d]

[a] Faculty of Engineering, Hokkaido University, Sapporo 060-8628, Japan.
[b] Graduate School of Chemical Sciences and Engineering, Hokkaido University, Sapporo 060-8628, Japan.
[c] Department of Materials Science and Engineering, UC Berkeley, Berkeley, California 94720, USA
[d] Materials Sciences Division, Lawrence Berkeley National Laboratory, Berkeley, CA 94720, USA
[e] Department of Chemistry, School of Science, Tokyo Institute of Technology, Tokyo 152-8550, Japan

Supporting Information Placeholder

ABSTRACT: MgCr$_2$S$_4$ thiospinel is predicted to be a compelling Mg-cathode material, but its preparation via traditional solid-state synthesis methods has proven challenging. Wustrow *et al.* [*Inorg. Chem.* **57**, 14 (2018)] found that the formation of MgCr$_2$S$_4$ from MgS + Cr$_2$S$_3$ binaries requires weeks of annealing at 800 °C with numerous intermediate regrinds. The slow reaction kinetics of MgS + Cr$_2$S$_3$ → MgCr$_2$S$_4$ can be attributed to a miniscule thermodynamic driving force of $\Delta H = -2$ kJ/mol. Here, we demonstrate that the double ion-exchange metathesis reaction, MgCl$_2$ + 2 NaCrS$_2$ → MgCr$_2$S$_4$ + 2 NaCl, has a reaction enthalpy of $\Delta H = -47$ kJ/mol, which is thermodynamically driven by the large exothermicity of NaCl formation. Using this metathesis reaction, we successfully synthesized MgCr$_2$S$_4$ nanoparticles (< 200 nm) from MgCl$_2$ and NaCrS$_2$ precursors in a KCl flux at 500 °C in only 30 minutes. NaCl and other metathesis byproducts are then easily washed away by water. We rationalize the selectivity of MgCr$_2$S$_4$ in the metathesis reaction from the topology of the DFT-calculated pseudo-ternary MgCl$_2$-CrCl$_3$-Na$_2$S phase diagram. Our work helps to establish metathesis reactions as a powerful alternative synthesis route to inorganic materials that have otherwise small reaction energies from conventional precursors.

Introduction

Synthesis is the bedrock of inorganic materials chemistry,[1] serving as the first step to any further investigation into the structure-property relationships of materials. For ceramic materials, the traditional approach to solid-state synthesis involves grinding or milling precursors into powder form, followed by the firing of these precursors at high temperatures to form more complex materials. While this approach has led to the synthesis of many inorganic materials, it remains limited by a number of thermodynamic and kinetic constraints.[2] For example, the synthesis temperature should be high enough to facilitate fast diffusion and reaction kinetics, but low enough that the target compound does not melt or decompose. However, high temperatures also lead to the ripening of large particles, which eliminates interfaces and thereby reduces reaction kinetics.[3] Because of these often conflicting constraints, solid-state synthesis occasionally proceeds with slow reaction kinetics, non-equilibrium intermediates, or impurities,[4-6] which hinder the phase-pure synthesis of a desired target material.

One such material that has proven difficult to synthesize via traditional solid-state synthesis is $MgCr_2S_4$ thiospinel. In the search for Mg-ion cathode materials beyond the dominant Chevrel Mo_6S_8 phase,[7] Mg-thiospinels emerged as a promising class of compounds. Thiospinels benefit from a soft sulfur anion sublattice, which enhances Mg-ion mobility compared to oxides, and a spinel framework, which provides a favorable *tetrahedral→octahedral→tetrahedral* Mg^{2+} migration path with a low diffusion barrier.[8-9] $MgTi_2S_4$ was the first demonstrated Mg-thiospinel cathode material, successfully cycled at a C/5 rate at 60°C and achieving a specific energy density of 230 Wh kg^{-1}.[10-11] Our computational search for other candidate Mg-thiospinels found $MgCr_2S_4$ to possess compelling properties, including a high specific capacity (209 mA h g^{-1}) and energy density (244 Wh kg^{-1}), as well as a relatively low Mg-ion diffusion barrier of 540 meV.[10] Notably, $MgCr_2S_4$ was calculated with density functional theory (DFT) to fall upon the Mg-Cr-S convex hull, meaning it is thermodynamically stable with respect to competing compounds and should therefore be synthesizable.

Following this prediction, Wustrow *et al.* successfully synthesized $MgCr_2S_4$ through a traditional solid-state synthesis approach—although it was found to be a laborious reaction.[12] Starting from elemental (Mg + Cr + S) precursors, the binary sulfides, MgS and Cr_2S_3, formed rapidly upon heating. However, the subsequent reaction from MgS + Cr_2S_3 to ternary $MgCr_2S_4$ required holding at 800 °C for two weeks, with numerous intermediate regrinds. Notably, the reaction could not be accelerated by carrying out the synthesis at higher temperatures as $MgCr_2S_4$ decomposes into MgS and Cr_2S_3 above 900 °C. Although

MgCr$_2$S$_4$ is indeed a thermodynamically stable compound, we calculate the driving force (reaction enthalpy, ΔH_r) for its formation from MgS + Cr$_2$S$_3$ to be extremely small (-2 kJ/mol, **Eq. 1**). All reaction energies in this work utilize the publicly available DFT-calculated thermochemical data in the Materials Project database.[13] The slow reaction kinetics observed by Wustrow *et al.* can be attributed to this miniscule thermodynamic driving force. Moreover, long synthesis times can lead to the ripening of large MgCr$_2$S$_4$ particles, which reduces the interfacial area needed to activate Mg-ion intercalation and further slows down the reaction kinetics.

$$MgS + Cr_2S_3 \rightarrow MgCr_2S_4; \Delta H_r = -2 \text{ kJ/mol} \qquad (1)$$
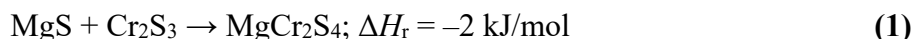
Metathesis reactions offer an intriguing synthesis route to solid-state materials with otherwise small reaction energies. In a metathesis reaction, an alkali or alkaline earth metal compound is combined with a metal halide, which drives a highly exothermic double ion-exchange reaction. For example, a compelling metathesis reaction for MgCr$_2$S$_4$ can be written as:

$$2 \text{ NaCrS}_2 + MgCl_2 \rightarrow MgCr_2S_4 + 2 \text{ NaCl}; \Delta H_r = -47 \text{ kJ/mol} \qquad (2)$$
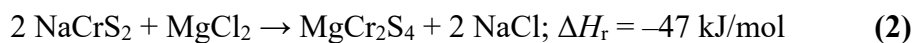
The >20× increase in thermodynamic driving force from $\Delta H_r = -2$ kJ/mol to -47 kJ/mol is because Na$^+$ and Cl$^-$ are separated in the precursors but rejoined to form NaCl on the product side. Along with a dramatic increase in reaction enthalpy, other advantages afforded by metathesis reactions include faster reaction kinetics and the potential formation of nanocrystals and porous materials[14]. Not only can metathesis reactions be used to synthesize stable materials with otherwise small reaction energies, the increased thermodynamic driving force and fast reaction kinetics also affords the synthesis of metastable materials,[15] as were previously demonstrated on nitrides,[14, 16-18] sulfides,[14, 19-20] and oxides.[21-23] Motivated by the metathesis reaction shown in **Eq. 2**, we designed a two-step sequential metathesis reaction to synthesize MgCr$_2$S$_4$, as visualized in **Scheme 1**.
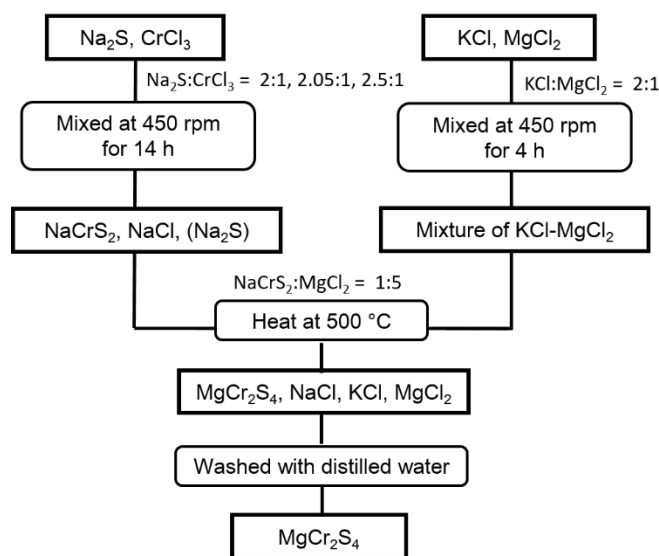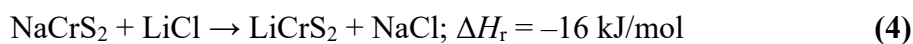
Scheme 1. Two-step metathesis flux synthesis of MgCr$_2$S$_4$.

Results

In the first reaction, we ball milled CrCl$_3$ and Na$_2$S to form NaCrS$_2$ (**Eq. 3**). This reaction is highly exothermic ($\Delta H_r = -359$ kJ/mol) and proceeds even without external heating.

$$CrCl_3 + 2Na_2S \rightarrow NaCrS_2 + 3NaCl; \Delta H_r = -359 \text{ kJ/mol} \qquad (3)$$
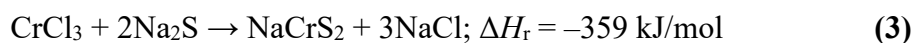
We next heated the byproducts from **Eq. 3** in a KCl-MgCl$_2$ flux in a nitrogen atmosphere (**Eq. 2**). We chose to conduct the reaction in a mixed chloride flux media in order to increase the diffusion kinetics of the reaction, which can in-turn reduce the temperature and time required for synthesis. Among LiCl, NaCl, and KCl flux chemistries, we disqualified a LiCl flux because the ion-exchange reaction of NaCrS$_2$ with LiCl has a favorable driving force to form LiCrS$_2$, which could compete with the formation of MgCr$_2$S$_4$ (**Eq. 4**). We disqualified a NaCl flux, as this may hinder the forward reaction to forming MgCr$_2$S$_4$ (**Eq. 2**) by Le Chatelier's principle. The formation of KCrS$_2$ from NaCrS$_2$ + KCl is not thermodynamically favorable (**Eq. 5**), and therefore KCl emerges as the optimal flux media.

$$NaCrS_2 + LiCl \rightarrow LiCrS_2 + NaCl; \Delta H_r = -16 \text{ kJ/mol} \qquad (4)$$

$$NaCrS_2 + KCl \rightarrow KCrS_2 + NaCl; \Delta H_r = +33 \text{ kJ/mol} \qquad (5)$$

These reaction thermodynamics are also straightforward to evaluate using the Materials Project Reaction Energy calculator, which can help guide the rational design of flux chemistries. To prepare the KCl-MgCl$_2$ flux, we chose the eutectic composition of KCl:MgCl$_2$ ~2:1,[24] which reduces the flux melting point to below 450 °C.

We synthesized NaCrS$_2$ in a reaction between CrCl$_3$ and Na$_2$S by ball-milling at 450 rpm in a zirconia jar with zirconia milling media. We tried three molar ratios for CrCl$_3$:Na$_2$S—1:2 (stoichiometric), 1:2.05 (2.5% Na$_2$S excess), and 1:2.5 (25% Na$_2$S excess)—producing NaCrS$_2$ and NaCl (**Eq. 3**). In the second step, the ball-milled mixture of NaCrS$_2$ and NaCl were placed in a carbon crucible together with the MgCl$_2$-KCl flux at a molar ratio of NaCrS$_2$:MgCl$_2$ = 1:5. The reaction was performed at 500 °C for 30 minutes in an inert nitrogen atmosphere. After cooling, the synthesized products were washed with distilled water and centrifuged in air to remove the flux and excess MgCl$_2$ and Na$_2$S. **Figure 1** shows the XRD characterization of the synthesis products. The ball-milling of Na$_2$S and CrCl$_3$ indeed produced NaCrS$_2$ with NaCl byproduct, as anticipated from **Eq. 3**. The reaction of NaCrS$_2$ + NaCl in a MgCl$_2$-KCl flux resulted in MgCr$_2$S$_4$, Cr$_2$S$_3$ and MgO, where the ratios of these products varied with the Na$_2$S excess in the precursor (**Figure 1**). For a stoichiometric ratio of CrCl$_3$:Na$_2$S = 1:2, we observe a coexistence of Cr$_2$S$_3$ and MgCr$_2$S$_4$. When we include Na$_2$S excess in the synthesis of NaCrS$_2$ (**Eq. 3**), the Cr$_2$S$_3$ impurity from the flux reaction is diminished. With 25% Na$_2$S excess, the reaction yields nearly phase-pure MgCr$_2$S$_4$.

All metathesis byproducts and flux media (KCl, NaCl, MgCl$_2$, Na$_2$S) and any possibly synthesized MgS are soluble in water and were removed from the system by washing with distilled water. Although our final product yields MgCr$_2$S$_4$ as the dominant phase, it contains MgO as a minor impurity. These reactions were conducted in inert nitrogen atmosphere, suggesting the incorporation of oxygen in MgO may have arisen from washing with water. To examine the effect of washing with water, we performed the same synthesis reaction of NaCrS$_2$ with MgBr$_2$-KBr flux, with excess MgBr$_2$ and Na$_2$S, and subsequently removed metathesis products by washing with anhydrous methanol. In the MgBr$_2$ synthesis, MgO still forms as an impurity phase, in fact with even larger phase fraction than when synthesized in the MgCl$_2$-KCl flux (**Figure S1**). This suggests that the oxygen does not originate from the water. Oxygen impurities may have therefore already existed in the MgCl$_2$ or MgBr$_2$ precursors, or from a low, but non-zero, p_{O2} and/or p_{H2O} in the nitrogen atmosphere.
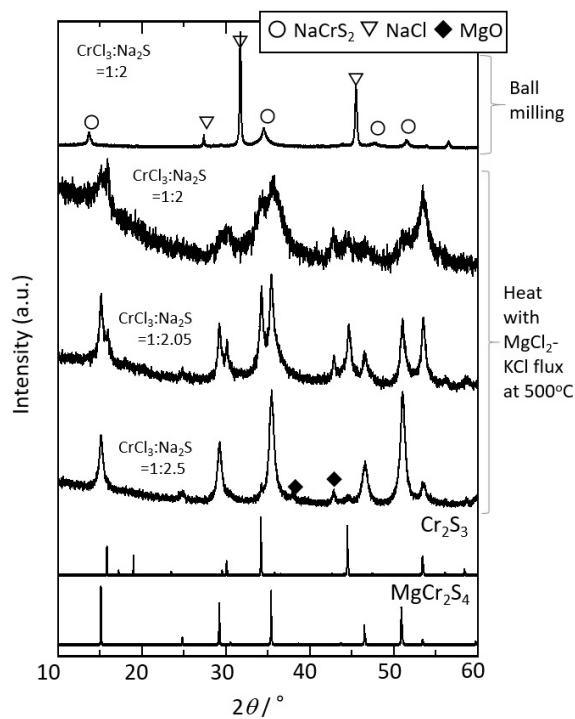
Figure 1. XRD patterns of $NaCrS_2$ powder synthesized via ball milling from $CrCl_3$ and Na_2S, and $MgCr_2S_4$ powder synthesized by $NaCrS_2$ and $MgCl_2$-KCl flux at 500 °C and subsequent wash with water. Different molar ratios of $CrCl_3$:Na_2S were utilized for producing $MgCr_2S_4$.

Rietveld refinement of $MgCr_2S_4$ synthesized from Na_2S and $MgCl_2$ excess (**Figure 2a**) shows that the lattice parameter of $MgCr_2S_4$ is 1.01426(12) nm, agreeing with the previously reported $MgCr_2S_4$ synthesized by high-temperature solid-state synthesis (1.01415(2) nm).[12] Rietveld refinement shows no inversion between Mg and Cr sites in the spinel structure. **Figure 2b** shows the STEM images and corresponding EDX mapping of $MgCr_2S_4$ particles synthesized via metathesis reactions with Na_2S and $MgCl_2$ excess. The as-synthesized particles are 50-200 nm in size and 20-50 nm in thickness. The relative surface area of powder by N_2 absorption is found to be 5.45 m^2 g^{-1}. Such small particles cannot be obtained by conventional high-temperature ceramic synthesis, demonstrating an additional advantage of metathesis synthesis routes. The molar ratio of Mg/Cr/S determined by EDX of the product is 1/2.4/4.1, which is close to the stoichiometric ratio of $MgCr_2S_4$. EDX mapping showed homogeneously distributed Mg and Cr, further supporting the formation of $MgCr_2S_4$.
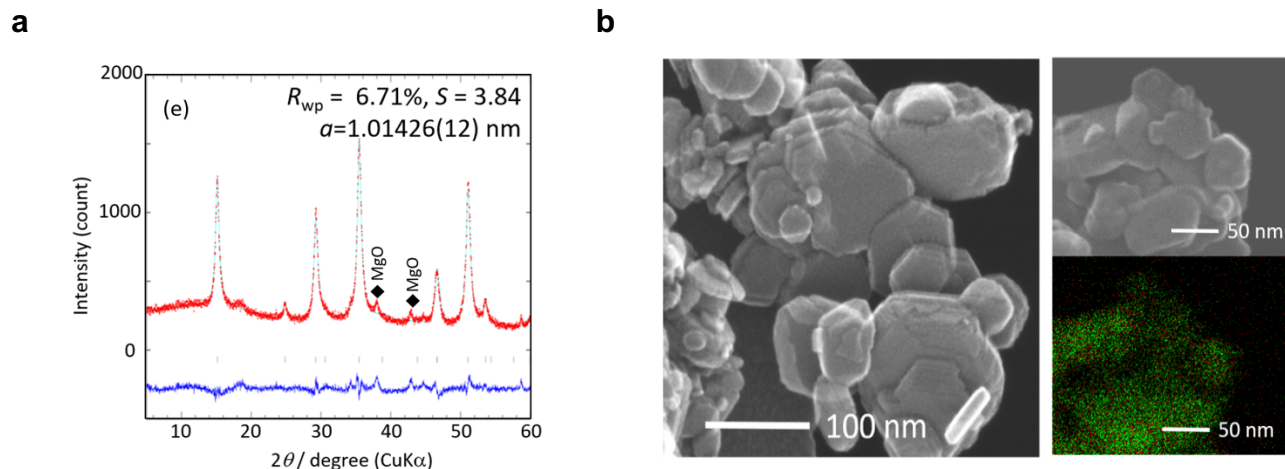
Figure 2. a) Rietveld profile of $MgCr_2S_4$ synthesized with excess Na_2S. Residual is shown as the blue line. **b)** STEM image of $MgCr_2S_4$ platelet particles. Right side is STEM and EDX mapping: red and green signals represent Mg and Cr signals, respectively.

The electronic properties of $MgCr_2S_4$ are an important consideration for Mg-ion battery performance and photochemical applications because Cr_2S_3 has been reported as *n*- and *p*-type semiconductor (band gap, $E_g = 0.8$ eV). [25] We measured the optical band gap of $MgCr_2S_4$ using diffuse reflectance spectroscopy (**Supporting Information**), which we estimate from the Tauc-plot to be 2.2 eV (**Figure S2**). By means of Mott–Schottky plot analysis (**Figure S3**), $MgCr_2S_4$ is shown to be an *n*-type semiconductor with a flat-band potential of ca. –0.6 V vs. Ag/AgCl at pH 7.0, indicating it may also be a candidate for H_2 evolution photocatalysts under visible light radiation.

Discussion

The accelerated formation of $MgCr_2S_4$ during metathesis (~30 minutes) compared with solid-state synthesis (~2 weeks) can be rationalized from the thermodynamic topology of each synthesis space. **Figure 3a** shows the ternary phase diagram for Mg-Cr-S, and **Figure 3b** shows a pseudo-ternary phase diagram for $MgCl_2$-$CrCl_3$-Na_2S, which is a slice of the larger 5-component Mg-Cr-S-Na-Cl phase diagram. The colorbar illustrates the 'depth' of the convex hull, corresponding to the reaction energy at each composition relative to the precursor endpoints. Even though $MgCr_2S_4$ has a very favorable formation enthalpy of –1.289 eV/atom, MgS and Cr_2S_3 also have very negative formation enthalpies of –1.76 and –1.097 eV/atom, respectively. In the Mg-Cr-S phase diagram, the deepest point is at the MgS composition, meaning MgS acts as a thermodynamic 'sink' in the traditional ceramic synthesis and explains why MgS

tends to persist during the traditional ceramic synthesis. **Figure 3c** further depicts the tiny energy gain to form $MgCr_2S_4$ along the MgS-Cr_2S_3 reaction tie-line, which further underlies the slow reaction kinetics.

On the other hand, the $MgCl_2$-$CrCl_3$-Na_2S metathesis phase diagram exhibits a qualitatively different thermodynamic topology. Here, each Mg-Cr-S composition must also be accompanied by a stoichiometrically-balanced amount of NaCl, which modifies the reaction energies at each composition in the pseudo-ternary space. $MgCr_2S_4$ is balanced by 8 NaCl, whereas MgS is balanced by 2 NaCl, $NaCrS_2$ by 3 NaCl, and Cr_2S_3 by 6 NaCl. In the $MgCl_2$-$CrCl_3$-Na_2S phase diagram, the inclusion of NaCl shifts the deepest thermodynamic point from MgS to $MgCr_2S_4$ + Cr_2S_3, which are indeed the observed reaction products in **Figure 1** when synthesized without Na_2S excess. The metathesis route therefore enhances the selective synthesis of $MgCr_2S_4$ by relocating the thermodynamic sink in composition space. Furthermore, because S is tied up with Cr in the $NaCrS_2$ precursor, MgS is unlikely to form in the metathesis reaction, as this would require $NaCrS_2$ decomposition and subsequent reaction of S with the $MgCl_2$ flux.

By increasing the amount of Na_2S excess in the precursor, the diffraction peaks of $MgCr_2S_4$ became dominant and the Cr_2S_3 impurity is eliminated (**Figure 1**). This can be rationalized from Le Chatlier's principle, as illustrated in **Figure 3c**, where Cr_2S_3 impurities react with excess Na_2S as well as excess $MgCl_2$ from the flux, which further drives the reaction towards the $MgCr_2S_4$ product side. The reaction between Cr_2S_3, $MgCl_2$ and Na_2S (**Figure 3c**, orange line) has larger thermodynamic driving force than that between $NaCrS_2$ and $MgCl_2$ (**Figure 3c**, blue line). Operating with excess Na_2S and $MgCl_2$ therefore encourages the formation of $MgCr_2S_4$ at the expense of the Cr_2S_3 impurity. Wustrow *et al.* used a similar strategy in the traditional solid-state synthesis route, providing excess MgS to react with Cr_2S_3 impurities in order to achieve high-purity $MgCr_2S_4$.
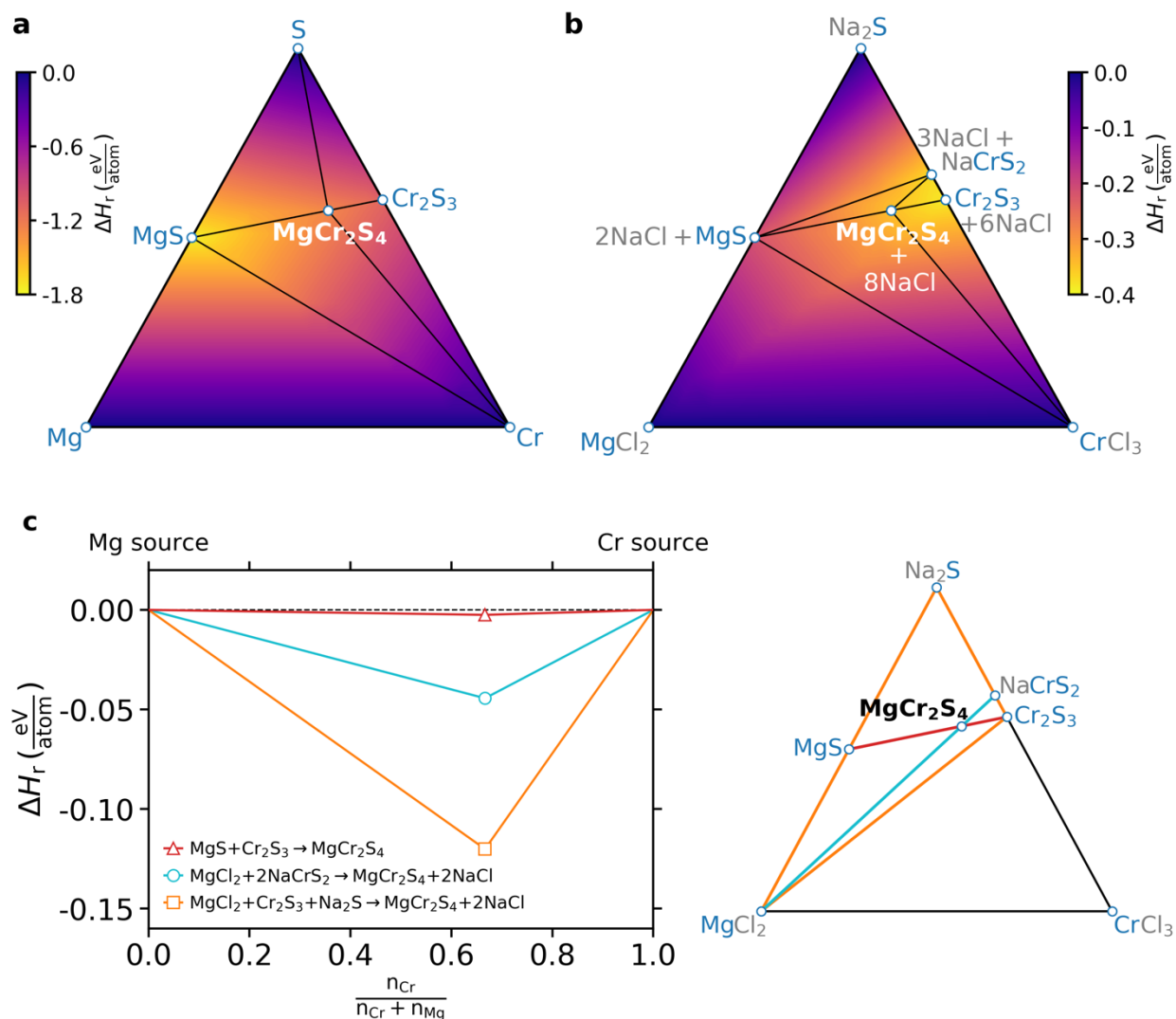
Figure 3. Ternary phase diagrams for **a)** Mg-Cr-S, corresponding to a traditional ceramic synthesis reaction and **b)** MgCl$_2$-CrCl$_3$-Na$_2$S, corresponding to a metathesis reaction. The color bar indicates the reaction enthalpy between the corners of each triangle and the convex hull, which represents the minimum energy phase or mixture of phases at each composition. For **b)**, ΔH_r is calculated by considering the formation of NaCl where appropriate and therefore is a pseudo-ternary representation of the quinary Mg-Cr-S-Na-Cl chemical space. **c)** Driving force for MgCr$_2$S$_4$ from three routes, highlighted by their color in the corresponding pseudo-ternary phase diagram. The reaction relevant to ceramic synthesis (**Eq. 1**) is shown in red, the metathesis reaction (**Eq. 3**) is shown in blue, and the reaction that proceeds with excess Na$_2$S + MgCl$_2$, and consumes impurity Cr$_2$S$_3$, is shown in orange.

Conclusions

In summary, we demonstrated metathesis reactions as a powerful synthesis route to inorganic materials with otherwise small thermodynamic driving forces. The formation of NaCl as a byproduct not only increases the reaction enthalpy of forming the target phase, but shifts the topology of the phase diagram,

changing the composition of the deepest point of the convex hull and thereby enhancing structure-selectivity. Here, we demonstrated the metathesis synthesis of $MgCr_2S_4$ in only 30 minutes at 500 °C, in contrast to a two-week traditional ceramic synthesis at 800 °C with multiple intermediate regrinds. Furthermore, the synthesized $MgCr_2S_4$ particles were 100-200 nm in size, which is a smaller particle size than would be realized in a direct solid-state ceramic synthesis. Our metathesis synthesis of $MgCr_2S_4$ enables the future studies of its electrochemical performance for Mg-battery and photocatalytic applications.

From a more general perspective, the concept of the metathesis reaction broadens how we evaluate synthesis and synthesizability. Traditionally, we take an 'addition' approach to materials synthesis, where one mixes together simple precursors to form a more complex multicomponent material. In the metathesis route, the reactions are driven by stable but removable byproducts, which include but are not limited to alkali metal halides. For example, the reaction of chlorides/oxides with H_2S or NH_3 gas could also be used to synthesize sulfides, oxysulfides, nitrides and oxynitrides by generating HCl/H_2O gas as a byproduct.[26-28] Inclusion of these extra species into the phase diagram changes the relevant chemical reactions and drastically modifies the thermodynamic landscape. The additional degrees of freedom afforded by including these extra elements into the phase diagram opens up a vast and promising design space for clever metathesis reactions. These candidate metathesis reactions can be rapidly screened and evaluated using publicly available DFT thermochemical data.

Methods

The thermodynamics for all reactions discussed in this work are obtained from density functional theory calculations available in the Materials Project database.[13] The syntheses were performed by two-step metathesis reactions. First, the reaction between $CrCl_3$ (99 %, Sigma-Aldrich) and Na_2S (Nagao & Co., Ltd.) with the molar ratio of 1:2, 1:2.05 (2.5 %Na_2S excess), and 1:2.5 (25 %Na_2S excess) were performed to produce $NaCrS_2$ and $NaCl$. This reaction was performed by ball-milling at 350 rpm with zirconia pot and ball. The second step was the reaction of $NaCrS_2$ with $MgCl_2$. This reaction was performed at 500 °C for 30 minutes in an inert atmosphere. The ball-milled mixture of $NaCrS_2$ and $NaCl$ was placed in a carbon crucible together with an $MgCl_2$-KCl flux: $MgCl_2$ (99.9 %, Kojundo Chemical Laboratory), KCl (>99.5 %, Wako Chemicals). The molar ratio of $NaCrS_2$ to $MgCl_2$ was 1:5. After cooling, the synthesized products were washed with distilled water and centrifuged in ambient atmosphere to remove flux and excess $MgCl_2$ and Na_2S. XRD diffraction was measured by MiniFlex 600 (Rigaku). Composition

ratio was determined by EDX equipped by scanning electron microscopy (SEM: TM3030). Morphology was observed by scanning transmission electron microscopy (STEM: Hitachi HD-2000). The diffuse reflectance spectra of $MgCr_2S_4$ were measured using a UV-vis spectrophotometer (JASCO V-750) at room temperature. Mott-Schottky plot measurements were conducted using an ALS760Es electrochemical analyzer (BAS) at room temperature. The electrochemical cell was made of Pyrex glass and was a three-electrode-type system using Pt wire and an Ag/AgCl electrode (in saturated KCl aqueous solution) as the counter and reference electrodes, respectively. The pH of the electrolyte solution was adjusted to be 7.0 by mixing $NaH_2PO_4 \cdot 2H_2O$ (99.0–102.0 %, Kanto Chemical) and $Na_2HPO_4 \cdot 12H_2O$ (>99.0 %, Kanto Chemical), while keeping the total phosphate concentration of 0.1 M.

ASSOCIATED CONTENT

Supporting Information

XRD patterns using an alternative $MgBr_2$-KBr flux and electronic property characterization of the as-synthesized $MgCr_2S_4$.

AUTHOR INFORMATION

Corresponding Authors

Akira Miura: amiura@eng.hokudai.ac.jp
Wenhao Sun: wenhaosun@lbl.gov

ACKNOWLEDGMENT

REFERENCES

1.   Kanatzidis, M. G.; Poeppelmeier, K. R.; Bobev, S.; Guloy, A. M.; Hwu, S.-J.; Lachgar, A.; Latturner, S. E.; Raymond; Schaak, E.; Seo, D.-K.; Sevov, S. C.; Stein, A.; Dabrowski, B.; Greedan, J. E.; Greenblatt, M.; Grey, C. P.; Jacobson, A. J.; Keszler, D. A.; Li, J.; Subramanian, M. A.; Xia, Y.; Cagin, T.; Häussermann, U.; Hughbanks, T.; Mahanti, S. D.; Morgan, D.; Seo, D.-K.; Spaldin, N. A.; Buhro, W. E.; Giammar, D. E.; Hollingsworth, J. A.; Johnson, D. C.; Nozik, A. J.; Peng, X.; Bedard, R. L.; Brese, N. E.; Cao, G.; Dhingra, S. S.; Kagan, C. R.; Mitzi, D. B.; Geselbracht, M. J.; Lisensky, G. C.; Lufaso, M. W.; Maggard, P. A.; Michael, O. K.; Wilkinson, A. P.; zur Loye, H.-C.; Egami, T.; Greedan, J. E.; Hodges, J. P.; Martin, J. D.; Parise, J. B.; Toby, B. H.; Vanderah, T. A.; Burns, P. C.; Chan, J. Y.; Meyer, A. E.; Murray, C. B.; Ramirez, A. P.; Ward, M. D.; Yu, L.; Alario-Franco, M. A.; Battle, P. D.; Bein, T.; Cahill, C. L.; Halasyamani, P. S.; Maignan, A.; Seshadri, R., Report from the third workshop on future directions of solid-state chemistry: The status of solid-state chemistry and its impact in the physical sciences. *Prog. Solid State Chem*. **2008,** *36* (1), 1-133.

2.   DiSalvo, F. J., Solid-State Chemistry: A Rediscovered Chemical Frontier. *Science* **1990,** *247* (4943), 649-655.

3.   German, R. M., Sintering. In *Encyclopedia of Materials: Science and Technology*, Buschow, K. H. J.; Cahn, R. W.; Flemings, M. C.; Ilschner, B.; Kramer, E. J.; Mahajan, S.; Veyssière, P., Eds. Elsevier: Oxford, 2001; pp 8641-8643.

4.   Shoemaker, D. P.; Hu, Y.-J.; Chung, D. Y.; Halder, G. J.; Chupas, P. J.; Soderholm, L.; Mitchell, J. F.; Kanatzidis, M. G., In situ studies of a platform for metastable inorganic crystal growth and materials discovery. *Proceedings of the National Academy of Sciences* **2014,** *111* (30), 10922.

5.   Jiang, Z.; Ramanathan, A.; Shoemaker, D. P., In situ identification of kinetic factors that expedite inorganic crystal formation and discovery. *Journal of Materials Chemistry C* **2017,** *5* (23), 5709-5717.

6.   Haynes, A. S.; Stoumpos, C. C.; Chen, H.; Chica, D.; Kanatzidis, M. G., Panoramic Synthesis as an Effective Materials Discovery Tool: The System Cs/Sn/P/Se as a Test Case. *J. Am. Chem. Soc*. **2017,** *139* (31), 10814-10821.

7.   Aurbach, D.; Lu, Z.; Schechter, A.; Gofer, Y.; Gizbar, H.; Turgeman, R.; Cohen, Y.; Moshkovich, M.; Levi, E., Prototype systems for rechargeable magnesium batteries. *Nature* **2000,** *407* (6805), 724-727.

8.	Rong, Z.; Malik, R.; Canepa, P.; Sai Gautam, G.; Liu, M.; Jain, A.; Persson, K.; Ceder, G., Materials Design Rules for Multivalent Ion Mobility in Intercalation Structures. *Chem. Mater.* **2015,** *27* (17), 6016-6021.

9.	Liu, M.; Rong, Z.; Malik, R.; Canepa, P.; Jain, A.; Ceder, G.; Persson, K. A., Spinel compounds as multivalent battery cathodes: a systematic evaluation based on ab initio calculations. *Energy & Environmental Science* **2015,** *8* (3), 964-974.

10.	Liu, M.; Jain, A.; Rong, Z.; Qu, X.; Canepa, P.; Malik, R.; Ceder, G.; Persson, K. A., Evaluation of sulfur spinel compounds for multivalent battery cathode applications. *Energy & Environmental Science* **2016,** *9* (10), 3201-3209.

11.	Sun, X.; Bonnick, P.; Duffort, V.; Liu, M.; Rong, Z.; Persson, K. A.; Ceder, G.; Nazar, L. F., A high capacity thiospinel cathode for Mg batteries. *Energy & Environmental Science* **2016,** *9* (7), 2273-2277.

12.	Wustrow, A.; Key, B.; Phillips, P. J.; Sa, N.; Lipton, A. S.; Klie, R. F.; Vaughey, J. T.; Poeppelmeier, K. R., Synthesis and Characterization of MgCr2S4 Thiospinel as a Potential Magnesium Cathode. *Inorg. Chem.* **2018,** *57* (14), 8634-8638.

13.	Jain, A.; Ong, S. P.; Hautier, G.; Chen, W.; Richards, W. D.; Dacek, S.; Cholia, S.; Gunter, D.; Skinner, D.; Ceder, G.; Persson, K. A., Commentary: The Materials Project: A materials genome approach to accelerating materials innovation. *APL Materials* **2013,** *1* (1), 011002.

14.	Wiley, J. B.; Kaner, R. B., Rapid Solid-State Precursor Synthesis of Materials. *Science* **1992,** *255* (5048), 1093-1097.

15.	Sun, W.; Dacek, S. T.; Ong, S. P.; Hautier, G.; Jain, A.; Richards, W. D.; Gamst, A. C.; Persson, K. A.; Ceder, G., The thermodynamic scale of inorganic crystalline metastability. *Sci. Adv.* **2016,** *2* (11), e1600225-e1600225.

16.	Odahara, J.; Sun, W.; Miura, A.; Rosero-Navarro, N. C.; Nagao, M.; Tanaka, I.; Ceder, G.; Tadanaga, K., Self-Combustion Synthesis of Novel Metastable Ternary Molybdenum Nitrides. *ACS Materials Letters* **2019,** *1* (1), 64-70.

17.	Miura, A.; Rosero-Navarro, C.; Masubuchi, Y.; Higuchi, M.; Kikkawa, S.; Tadanaga, K., Nitrogen-Rich Manganese Oxynitrides with Enhanced Catalytic Activity in the Oxygen Reduction Reaction. *Angew. Chem. Int. Ed. Engl.* **2016,** *55* (28), 7963-7.

18.	Rognerud, E. G.; Rom, C. L.; Todd, P. K.; Singstock, N. R.; Bartel, C. J.; Holder, A. M.; Neilson, J. R., Kinetically Controlled Low-Temperature Solid-State Metathesis of Manganese Nitride Mn3N2. *Chem. Mater.* **2019,** *31* (18), 7248-7254.

19.	Martinolich, A. J.; Kurzman, J. A.; Neilson, J. R., Circumventing Diffusion in Kinetically Controlled Solid-State Metathesis Reactions. *J. Am. Chem. Soc.* **2016,** *138* (34), 11031-7.

20.	Martinolich, A. J.; Neilson, J. R., Toward Reaction-by-Design: Achieving Kinetic Control of Solid State Chemistry with Metathesis. *Chem. Mater.* **2017,** *29* (2), 479-489.

21.	Shannon, R. D.; Rogers, D. B.; Prewitt, C. T., Chemistry of noble metal oxides. I. Syntheses and properties of ABO2 delafossite compounds. *lnorg. Chem.* **1971,** *10* (4), 713-718.

22.	Todd, P. K.; Neilson, J. R., Selective formation of yttrium manganese oxides through kinetically competent assisted metathesis reactions. *J. Am. Chem. Soc.* **2019**.

23.	Todd, P. K.; Smith, A. M. M.; Neilson, J. R., Yttrium Manganese Oxide Phase Stability and Selectivity Using Lithium Carbonate Assisted Metathesis Reactions. *Inorg. Chem.* **2019,** *58* (22), 15166-15174.

24.	Grjotheim, K.; Holm, J. L.; Røtnes, M., The Phase Diagrams of the Systems NaCl-MgCl2 and KCl-MgCl2. *Acta Chem. Scand.* **1972,** *26*, 3802-3803.

25.	Anedda, A.; Fortin, E.; Ledda, F.; Serpi, A., Photoelectrical properties of Cr2S3. *physica status solidi (b)* **1982,** *114* (2), K143-K146.

26.	Elder, S. H.; Doerrer, L. H.; Disalvo, F. J.; Parise, J. B.; Guyomard, D.; Tarascon, J. M., LiMoN$_2$ - the 1st metallic layered nitride. *Chem. Mater.* **1992,** *4* (4), 928-937.

27.	Miura, A.; Tadanaga, K.; Magome, E.; Moriyoshi, C.; Kuroiwa, Y.; Takahiro, T.; Kumada, N., Octahedral and trigonal-prismatic coordination preferences in Nb-, Mo-, Ta-, and W-based ABX$_2$ layered oxides, oxynitrides, and nitrides. *J. Solid State Chem.* **2015,** *229*, 272-277.

28.	Kageyama, H.; Hayashi, K.; Maeda, K.; Attfield, J. P.; Hiroi, Z.; Rondinelli, J. M.; Poeppelmeier, K. R., Expanding frontiers in materials chemistry and physics with multiple anions. *Nat Commun* **2018,** *9* (1), 772.

Table of contents figure
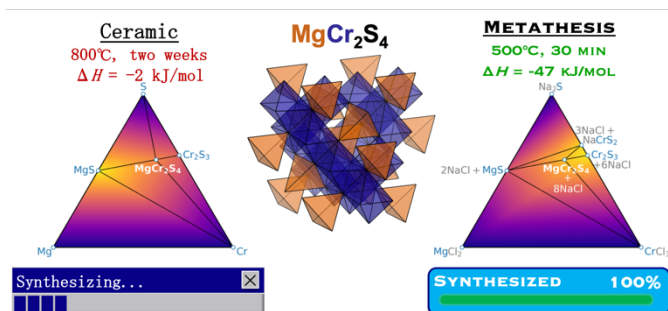
Supporting Information: Selective metathesis synthesis of MgCr₂S₄ by control of thermodynamic driving forces

Akira Miura,[a*] Hiroki Ito,[b] Christopher J. Bartel,[c] Wenhao Sun,[d*] Nataly Carolina Rosero-Navarro,[a] Kiyoharu Tadanaga,[a] Hiroko Nakata,[e] Kazuhiko Maeda,[e] Gerbrand Ceder[c,d]

[a] Faculty of Engineering, Hokkaido University, Sapporo 060-8628, Japan.
[b] Graduate School of Chemical Sciences and Engineering, Hokkaido University, Sapporo 060-8628, Japan.
[c] Department of Materials Science and Engineering, UC Berkeley, Berkeley, California 94720, USA
[d] Materials Sciences Division, Lawrence Berkeley National Laboratory, Berkeley, CA 94720, USA
[e] Department of Chemistry, School of Science, Tokyo Institute of Technology, Tokyo 152-8550, Japan
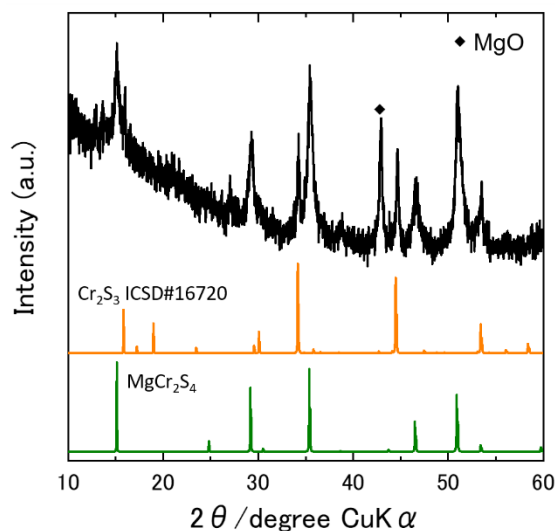
Figure S1. XRD pattern of $MgCr_2S_4$ synthesized from $NaCrS_2$ and $MgBr_2$-KBr flux with excess Na_2S and subsequent washing with methanol.
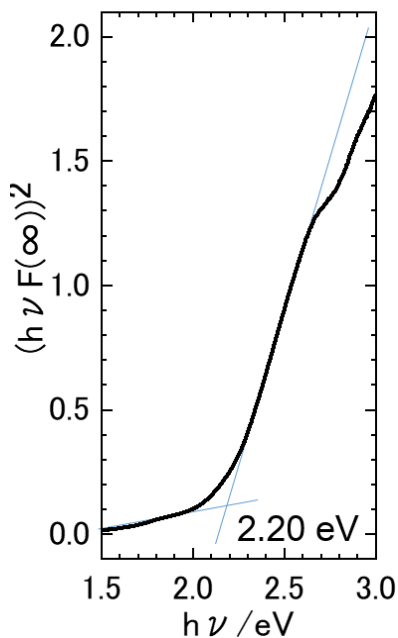
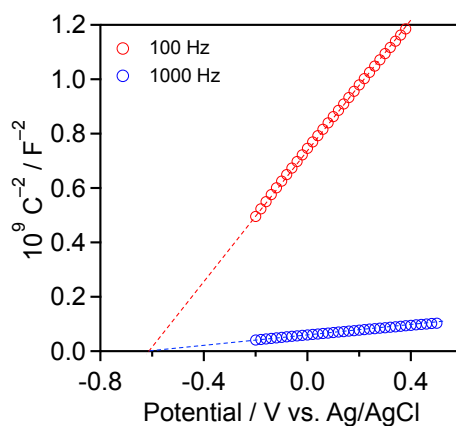**Figure S2**. Tauc plot of $MgCr_2S_4$ powders synthesized under Na_2S excess condition.

Figure S3. Mott–Schottky plot of the $MgCr_2S_4$/FTO electrode measured in aqueous NaH_2PO_4–Na_2HPO_4 solution (PO_4^{3-} = 0.1 M) at pH 7.0. The electrode was prepared by electrophoretic deposition in a 50 mL acetone solution (>99.5%, Kanto Chemical) containing 0.05 g $MgCr_2S_4$ powder (synthesized under Na_2S excess condition) and 10 mg iodine (>99.8%, Wako Pure Chemicals). Two parallel FTO electrodes were immersed in the solution with ca. 15 mm separation, and a 20 V bias was applied between them for 30 s using a potentiostat (PSW 80-13.5, GW Instek). The $MgCr_2S_4$-coated area was fixed ca. 1.5 cm × 3.5 cm.